Progress In Electromagnetics Research, Vol. 107, 239–252, 2010

MULTILEVEL GREEN'S FUNCTION INTERPOLATION METHOD SOLUTION OF VOLUME/SURFACE INTEGRAL EQUATION FOR MIXED CONDUCTING/BI-ISOTROPIC OBJECTS

Y. Shi, X. Luan, J. Qin, C. J. Lv, and C. H. Liang

School of Electronic Engineering
Xidian University
Xi'an 710071, China

Abstract—This paper proposes a multilevel Green's function interpolation method (MLGFIM) to solve electromagnetic scattering from objects comprising both conductor and bi-isotropic objects using volume/surface integral equation (VSIE). Based on equivalence principle, the volume integral equation (VIE) in terms of volume electric and magnetic flux densities and surface integral equation (SIE) in terms of surface electric current density are first formulated for inhomogeneous bi-isotropic and conducting objects, respectively, and then are discretized using the method of moments (MoM). The MLGFIM is adopted to speed up the iterative solution of the resultant equation and reduces the memory requirement. Numerical examples are presented to show good accuracy and versatility of the proposed algorithm in dealing with a wide array of scattering problems.

1. INTRODUCTION

With the rapid development of material technology, complex media with a variety of constitutive relationships have attracted increasing attention, and therefore a need for accurate and efficient analysis of electromagnetic wave propagation and scattering properties in those media has been promoted. Among these new materials, bi-isotropic medium [1] has emerged as one of the most promising topics in electromagnetic community. Many potential applications of bi-isotropic materials in microwave and millimeter devices have been

Received 2 June 2010, Accepted 4 August 2010, Scheduled 10 August 2010
Corresponding author: Y. Shi (shiyan@mail.xidian.edu.cn).

proposed such as polarization rotators, electromagnetic interference shielding and radar absorbers [2]. Analysis of electromagnetic properties of bi-isotropic materials is challenging due of its constitutive relationships enforcing an additional coupling between the electric and magnetic fields. In recent years, several efforts have been made to develop various numerical techniques to study their scattering properties [3–10]. However these methods suffer from tremendously high computational cost.

Recent developments in fast algorithms have alleviated this problem to some extent. Multilevel fast multipole algorithm (MLFMA) [11–14], adaptive integral method (AIM) [15–17], sparse matrix canonical grid method (SMCG) [18, 19] and pre-corrected fast Fourier transform (PFFT) [20, 21] etc., have been proposed to fast calculate the field interaction with inhomogeneous isotropic media. More recently, a kernel independent approach, i.e., multilevel Green's function interpolation method (MLGFIM) [22–27] has been proposed to solve complex EM problems. It inherits the tree structure of the kernel dependent MLFMA and combines interpolation ideas of PFFT. To date, the MLGFIM has been successfully implemented for the solution to low-frequency and large-scale full-wave EM problems with computational complexities of $O(N)$ and $O(N \log N)$, respectively and all of memory complexities of $O(N)$.

In this paper, the MLGFIM is applied to accelerate the solution of the volume/surface integral equation (VSIE) for the composite conducting and bi-isotropic objects. The volume integral equation (VIE) and surface integral equation (SIE) are formulated to describe the inhomogeneous bi-isotropic and conducting objects, respectively. The resultant equations are converted into matrix equations by using the method of moments (MoM). The MLGFIM is utilized to reduce the memory requirement for matrix storage and to speed up the matrix-vector multiplication in iterative solution process. Numerical examples demonstrate the accuracy and versatility of the proposed approach.

2. FORMULATION

2.1. Volume/Surface Integral Equation

Consider an arbitrary structure that contains conducting and inhomogeneous bi-isotropic objects embedded in a homogeneous background medium of infinite extent with permittivity ε_0 and permeability μ_0, as shown in Fig. 1. The constitutive relationship

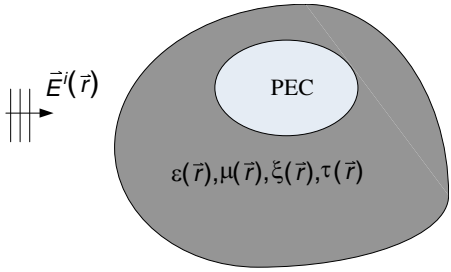

Figure 1. Geometry including mixed bi-isotropic and conducting objects.

in bi-isotropic media can be expressed as follows [1]:

$$\begin{aligned} \vec{D} &= \varepsilon_0\varepsilon_r\vec{E} + \xi\sqrt{\varepsilon_0\mu_0}\vec{H} \\ \vec{B} &= \mu_0\mu_r\vec{H} + \tau\sqrt{\varepsilon_0\mu_0}\vec{E} \end{aligned} \tag{1}$$

where the relative permittivity ε_r, the relative permeability μ_r and the bi-isotropic parameters ξ and τ are position dependent. If $\xi = \tau = 0$, (1) will reduce to the isotropic case. According to (1), we can get

$$\begin{aligned} \vec{E} &= c_{11}\vec{D} + c_{12}\vec{B} \\ \vec{H} &= c_{21}\vec{D} + c_{22}\vec{B} \end{aligned} \tag{2}$$

in which

$$\begin{aligned} c_{11} &= \frac{\chi_{JD}+1}{\varepsilon_0} = \frac{\mu_r}{\varepsilon_0}\frac{1}{\varepsilon_r\mu_r - \xi\tau} \\ c_{12} &= \frac{\chi_{JB}}{\varepsilon_0} = -\frac{1}{\sqrt{\varepsilon_0\mu_0}}\frac{\xi}{\varepsilon_r\mu_r - \xi\tau} \\ c_{21} &= \frac{\chi_{MD}}{\mu_0} = -\frac{1}{\sqrt{\varepsilon_0\mu_0}}\frac{\tau}{\varepsilon_r\mu_r - \xi\tau} \\ c_{22} &= \frac{\chi_{MB}+1}{\mu_0} = \frac{\varepsilon_r}{\mu_0}\frac{1}{\varepsilon_r\mu_r - \xi\tau} \end{aligned} \tag{3}$$

Substituting (2) into two curl equations of Maxwell's equations in sourceless region, we can obtain

$$\begin{aligned} \nabla\times\vec{H} &= -i\omega\vec{D} = -i\omega\varepsilon_0\vec{E} + i\omega\left[\chi_{JD}\vec{D} + \chi_{JB}\vec{B}\right] \\ \nabla\times\vec{E} &= i\omega\vec{B} = i\omega\mu_0\vec{H} - i\omega\left[\chi_{MD}\vec{D} + \chi_{MB}\vec{B}\right] \end{aligned} \tag{4}$$

Assuming

$$\begin{aligned}\vec{J}_V &= i\omega\left[\chi_{JD}\vec{D} + \chi_{JB}\vec{B}\right] \\ \vec{M}_V &= i\omega\left[\chi_{MD}\vec{D} + \chi_{MB}\vec{B}\right]\end{aligned} \tag{5}$$

(4) can be rewritten as

$$\begin{aligned}\nabla \times \vec{H} &= -i\omega\varepsilon_0\vec{E} + \vec{J}_V \\ \nabla \times \vec{E} &= i\omega\mu_0\vec{H} - \vec{M}_V\end{aligned} \tag{6}$$

From a microscopic viewpoint, $\vec{J}_V$ and $\vec{M}_V$ can be seen as equivalent volume electric and magnetic current densities [6]. In this scenario, using the equivalent principle scattered electric and magnetic fields $\vec{E}^s(\vec{r})$ and $\vec{H}^s(\vec{r})$ are the sum of fields radiated by equivalent electric current densities on the surface of conductor and fields radiated by equivalent electric and magnetic currents densities in bi-isotropic objects, i.e.,

$$\vec{E}^s\left(\vec{r}\right) = \vec{E}_S^s\left(\vec{r}\right) + \vec{E}_V^s\left(\vec{r}\right) \tag{7}$$

$$\vec{H}^s\left(\vec{r}\right) = \vec{H}_S^s\left(\vec{r}\right) + \vec{H}_V^s\left(\vec{r}\right) \tag{8}$$

where

$$\vec{E}_S^s\left(\vec{r}\right) = i\omega\vec{A}_S\left(\vec{r}\right) - \nabla\phi_S\left(\vec{r}\right) \tag{9}$$

$$\vec{H}_S^s\left(\vec{r}\right) = \frac{1}{\mu_0}\nabla \times \vec{A}_S\left(\vec{r}\right) \tag{10}$$

$$\vec{E}_V^s\left(\vec{r}\right) = i\omega\vec{A}_V\left(\vec{r}\right) - \nabla\phi_V\left(\vec{r}\right) - \frac{1}{\varepsilon_0}\nabla \times \vec{F}_V\left(\vec{r}\right) \tag{11}$$

$$\vec{H}_V^s\left(\vec{r}\right) = i\omega\vec{F}_V\left(\vec{r}\right) - \nabla\varphi_V\left(\vec{r}\right) + \frac{1}{\mu_0}\nabla \times \vec{A}_V\left(\vec{r}\right) \tag{12}$$

in which

$$\vec{A}_\alpha\left(\vec{r}\right) = \frac{\mu_0}{4\pi}\int\limits_\alpha G\left(\vec{r},\vec{r}'\right)\vec{J}_\alpha\left(\vec{r}'\right)d\alpha' \quad (\alpha = S, V) \tag{13}$$

$$\phi_\alpha\left(\vec{r}\right) = \frac{1}{i\omega 4\pi\varepsilon_0}\int\limits_\alpha G\left(\vec{r},\vec{r}'\right)\nabla' \cdot \vec{J}_\alpha\left(\vec{r}'\right)d\alpha' \tag{14}$$

$$\vec{F}_V\left(\vec{r}\right) = \frac{\varepsilon_0}{4\pi}\int\limits_V G\left(\vec{r},\vec{r}'\right)\vec{M}_V\left(\vec{r}'\right)dv' \tag{15}$$

$$\varphi_V\left(\vec{r}\right) = \frac{1}{i\omega 4\pi\mu_0}\int\limits_V G\left(\vec{r},\vec{r}'\right)\nabla'\cdot\vec{M}_V\left(\vec{r}'\right)dv' \tag{16}$$

$$G\left(\vec{r},\vec{r}'\right) = \frac{e^{ik\left|\vec{r}-\vec{r}'\right|}}{\left|\vec{r}-\vec{r}'\right|} \quad (k=\omega\sqrt{\mu_0\varepsilon_0}) \tag{17}$$

In bi-isotropic objects, the total electric and magnetic fields $\vec{E}^t\left(\vec{r}\right)$ and $\vec{H}^t\left(\vec{r}\right)$ are equal to the sum of the incident fields and scattered fields. Hence, the volume integral equations can be written as

$$\vec{E}^t\left(\vec{r}\right) = \vec{E}^i\left(\vec{r}\right) + \vec{E}^s\left(\vec{r}\right) \tag{18}$$

$$\vec{H}^t\left(\vec{r}\right) = \vec{H}^i\left(\vec{r}\right) + \vec{H}^s\left(\vec{r}\right) \quad \left(\vec{r}\in V\right) \tag{19}$$

On conducting surfaces, the tangential components of total electric fields vanish, i.e.,

$$\hat{n}\times\left[\vec{E}^i\left(\vec{r}\right) + \vec{E}^s\left(\vec{r}\right)\right] = 0 \quad \left(\vec{r}\in S\right) \tag{20}$$

in which $\hat{n}$ is the unit normal vector that points toward the exterior of conductor.

In order to solve VSIE (18)–(20), the scatterer is first approximately represented by a set of mesh cells of one-tenth of a wavelength. The zeroth order divergence conforming basis functions [28] defined on curvilinear hexahedral and quadrilateral elements are adopted as volume and surface basis functions, respectively. Substituting (2), (5) and (7)–(17) into (18)–(20) and applying Galerkin method, a linear system can be obtained as follows:

$$\begin{bmatrix} Z^{DD} & Z^{DB} & Z^{DS} \\ Z^{BD} & Z^{BB} & Z^{BS} \\ Z^{SD} & Z^{SB} & Z^{SS} \end{bmatrix}\begin{bmatrix} I^D \\ I^B \\ I^S \end{bmatrix} = \begin{bmatrix} V^D \\ V^B \\ V^S \end{bmatrix} \tag{21}$$

where

$$\begin{bmatrix} Z^{DD}_{mn} \\ Z^{DB}_{mn} \\ Z^{BD}_{mn} \\ Z^{BB}_{mn} \end{bmatrix} = -\begin{bmatrix} 1/i\omega\varepsilon_0 \\ 1/i\omega\varepsilon_0 \\ 1/i\omega\mu_0 \\ 1/i\omega\mu_0 \end{bmatrix}\int\limits_{v_m} dv\begin{bmatrix} \chi_{JD}\left(\vec{r}\right)+1 \\ \chi_{JB}\left(\vec{r}\right) \\ \chi_{MD} \\ \chi_{MB}\left(\vec{r}\right)+1 \end{bmatrix}\vec{f}_m\left(\vec{r}\right)\cdot\vec{f}_n\left(\vec{r}\right)$$

$$+\begin{bmatrix} i\omega\mu_0/4\pi \\ i\omega\mu_0/4\pi \\ i\omega\varepsilon_0/4\pi \\ i\omega\varepsilon_0/4\pi \end{bmatrix}\int\limits_{v_m} dv\int\limits_{v_n} dv'\begin{bmatrix} \chi_{JD}\left(\vec{r}'\right) \\ \chi_{JB}\left(\vec{r}'\right) \\ \chi_{MD}\left(\vec{r}'\right) \\ \chi_{MB}\left(\vec{r}'\right) \end{bmatrix}\vec{f}_m\left(\vec{r}\right)\cdot\vec{f}_n\left(\vec{r}'\right)G\left(\vec{r},\vec{r}'\right)$$

$$-\begin{bmatrix}1/i4\pi\omega\varepsilon_0\\1/i4\pi\omega\varepsilon_0\\1/i4\pi\omega\mu_0\\1/i4\pi\omega\mu_0\end{bmatrix}\int_{v_m}dv\int_{v_n}dv'\vec{f}_m(\vec{r})\cdot\nabla G\left(\vec{r},\vec{r}'\right)\left\{\nabla'\cdot\left(\begin{bmatrix}\chi_{JD}\left(\vec{\vec{r}}'\right)\\\chi_{JB}\left(\vec{\vec{r}}'\right)\\\chi_{MD}\left(\vec{\vec{r}}'\right)\\\chi_{MB}\left(\vec{\vec{r}}'\right)\end{bmatrix}\vec{f}_m\left(\vec{\vec{r}}'\right)\right)\right\}$$

$$+\begin{bmatrix}1/4\pi\\1/4\pi\\-1/4\pi\\-1/4\pi\end{bmatrix}\int_{v_m}dv\int_{v_n}dv'\begin{bmatrix}\chi_{MD}\left(\vec{\vec{r}}'\right)\\\chi_{MB}\left(\vec{\vec{r}}'\right)\\\chi_{JD}\left(\vec{\vec{r}}'\right)\\\chi_{JB}\left(\vec{\vec{r}}'\right)\end{bmatrix}\vec{f}_m\left(\vec{r}\right)\cdot\left[\vec{f}_n\left(\vec{\vec{r}}'\right)\times\nabla G\left(\vec{r},\vec{\vec{r}}'\right)\right] \quad (22)$$

$$\begin{bmatrix}Z_{mn}^{SD}\\Z_{mn}^{SB}\end{bmatrix}=\frac{i\omega\mu_0}{4\pi}\int_{s_m}ds\int_{v_n}dv'\begin{bmatrix}\chi_{JD}\left(\vec{\vec{r}}'\right)\\\chi_{JB}\left(\vec{\vec{r}}'\right)\end{bmatrix}\vec{f}_m\left(\vec{r}\right)\cdot\vec{f}_n\left(\vec{\vec{r}}'\right)G\left(\vec{r},\vec{\vec{r}}'\right)$$

$$-\frac{1}{i4\pi\omega\varepsilon_0}\int_{s_m}ds\int_{v_n}dv'\nabla\cdot\vec{f}_m\left(\vec{r}\right)\nabla'\cdot\left\{\begin{bmatrix}\chi_{JD}\left(\vec{\vec{r}}'\right)\\\chi_{JB}\left(\vec{\vec{r}}'\right)\end{bmatrix}\vec{f}_m\left(\vec{\vec{r}}'\right)\right\}G\left(\vec{r},\vec{\vec{r}}'\right)$$

$$+\frac{1}{4\pi}\int_{s_m}ds\int_{v_n}dv'\begin{bmatrix}\chi_{MD}\left(\vec{\vec{r}}'\right)\\\chi_{MB}\left(\vec{\vec{r}}'\right)\end{bmatrix}\vec{f}_m\left(\vec{r}\right)\cdot\left[\vec{f}_m\left(\vec{\vec{r}}'\right)\times\nabla G\left(\vec{r},\vec{\vec{r}}'\right)\right] \quad (23)$$

$$Z_{mn}^{DS}=\frac{i\omega\mu_0}{4\pi}\int_{v_m}dv\int_{s_n}ds'\vec{f}_m\left(\vec{r}\right)\cdot\vec{f}_n\left(\vec{\vec{r}}'\right)G\left(\vec{r},\vec{\vec{r}}'\right)$$

$$-\frac{1}{i4\pi\omega\varepsilon_0}\int_{v_m}dv\int_{s_n}ds'\nabla\cdot\vec{f}_m\left(\vec{r}\right)\nabla'\cdot\vec{f}_m\left(\vec{\vec{r}}'\right)G\left(\vec{r},\vec{\vec{r}}'\right) \quad (24)$$

$$Z_{mn}^{BS}=-\frac{1}{4\pi}\int_{v_m}dv\int_{s_n}ds'\vec{f}_m\left(\vec{r}\right)\cdot\left[\vec{f}_n\left(\vec{\vec{r}}'\right)\times\nabla G\left(\vec{r},\vec{\vec{r}}'\right)\right] \quad (25)$$

$$Z_{mn}^{SS}=\frac{i\omega\mu_0}{4\pi}\int_{s_m}ds\int_{s_n}ds'\vec{f}_m\left(\vec{r}\right)\cdot\vec{f}_n\left(\vec{\vec{r}}'\right)G\left(\vec{r},\vec{\vec{r}}'\right)$$

$$-\frac{1}{i4\pi\omega\varepsilon_0}\int_{s_m}dv\int_{s_n}ds'\nabla\cdot\vec{f}_m\left(\vec{r}\right)\nabla'\cdot\vec{f}_m\left(\vec{\vec{r}}'\right)G\left(\vec{r},\vec{\vec{r}}'\right) \quad (26)$$

$$\begin{bmatrix} V_m^D \\ V_m^B \end{bmatrix} = -\int_{v_m} d\vec{v} f_m(\vec{r}) \cdot \begin{bmatrix} \vec{E}^i(\vec{r}) \\ \vec{H}^i(\vec{r}) \end{bmatrix} \quad (27)$$

$$V_m^S = -\int_{s_m} ds \vec{f}_m(\vec{r}) \cdot \vec{E}^i(\vec{r}) \quad (28)$$

2.2. Multilevel Green's Function Interpolation Method

The memory requirement and computational complexity are $O\left(N^2\right)$, where N is the number of unknowns, when (21) is solved by using an iterative solver, for example generalized minimal residual method (GMRES) [29]. Hence, in order to improve computational efficiency and memory requirement, the MLGFIM will be implemented in this paper. We first enclose the entire object in a large cube, and then partition the large cube into eight smaller cubes. Each subcube is recursively subdivided into smaller cubes until the finest cubes satisfy the termination criterion. For two elements in same or adjacent finest cubes, their interaction is directly calculated; while the interaction between two elements in non-adjacent cubes is approximately calculated using multilevel interpolation technique [22–27].

By observing (22)–(26), we can find that matrix elements are composed of a general integral expression:

$$\Theta_{mn} = \gamma \int_{\alpha_m} d\alpha \int_{\beta_n} d\beta' \psi_m(\vec{r}) \phi_n\left(\vec{r}'\right) \Psi\left(\vec{r}, \vec{r}'\right) \quad (\alpha, \beta = V, S) \quad (29)$$

where $\psi_m(\vec{r})$, $\phi_n(\vec{r}')$ and $\Psi(\vec{r}, \vec{r}')$ are related to testing function, basis function and integral kernel, respectively. Here γ is a constant. For non-adjacent cubes, for example field cube G_u and source cube G_v, the integral kernel $\Psi(\vec{r}, \vec{r}')$ can be approximated using interpolation techniques as

$$\Psi\left(\vec{r}, \vec{r}'\right) = \sum_{p=1}^{K} \sum_{q=1}^{K} w_{G_u}^p(\vec{r}) w_{G_v}^q\left(\vec{r}'\right) \Psi\left(\vec{r}_{G_u,p}, \vec{r}'_{G_v,q}\right) \quad (30)$$

in which $w_{G_u}^p$ and $\vec{r}_{G_u,p}$ is the pth interpolation function and interpolation point in field cube G_u, respectively. Here K is the number

of interpolation points. Substituting (30) into (29), we can obtain

$$\Theta_{mn} = \gamma \sum_{p=1}^{K} \sum_{q=1}^{K} \left[\int_{\alpha_m} d\alpha \psi_m \left(\vec{r} \right) w_{G_u}^{p} \left(\vec{r} \right) \right] \Psi \left(\vec{r}_{G_u,p}, \vec{r}'_{G_v,q} \right) \left[\int_{\beta_n} d\beta' \phi_n \left(\vec{r}' \right) w_{G_v}^{q} \left(\vec{r}' \right) \right] \tag{31}$$

According to (31), we can see that the MLGFIM converts the direct interaction between field cube G_u and source cube G_v into three parts to fast calculate matrix-vector multiplication in the iterative solver. By handling the same or adjacent finest cubes and non-adjacent cubes separately as shown above, the MLGFIM can achieve its memory saving and CPU reduction [22–27]. The near interactions are directly calculated and saved in a sparse matrix, and therefore require $O(N)$ memory requirement; the far interactions are approximately computed using multilevel interpolation techniques with the storage also of $O(N)$. On the other hand, the computational complexity of near interactions is $O(N)$ while that of far interaction achieves $O(N \log N)$. All in all, memory requirement and computational complexity of MLGFIM are $O(N)$ and $O(N \log N)$, respectively. Detailed complexities analysis and interpolation techniques about the MLGFIM may refer to [22–27].

3. NUMERICAL RESULTS AND DISCUSSION

In this section, we present some numerical examples to demonstrate the accuracy and versatility of the proposed method. All calculations are performed on a computer with 3.0 GHz processor and 2.0 GB RAM. Here the QR factorization technique [30] is used to compress the Green's function matrix with low rank and the GMRES iteration method with a relative error norm of 0.001 is adopted for all simulations. Moreover, the sparse approximate inverse (SAI) [31] preconditioner is used to accelerate the convergence of iteration.

The first example considers a plane wave scattering from a homogeneous bi-isotropic cube with side length of $0.2\lambda_0$ where λ_0 is the wavelength in free space. The relative permittivity ε_r and permeability μ_r are 9 and 1, respectively and $\xi = \tau^* = 0.5 + i0.5$. Here, we use 1000 hexahedrons to discretize the cube and the resultant number of unknowns is 3300. A θ-polarized plane wave in the direction of $\theta = 180^\circ$ is incident on the cube and the co-polarized and cross-polarized bistatic RCS in the observation plane of $\phi = 0^\circ$ are calculated

as shown in Fig. 2. The results are in very good agreement with results in [6].

In the second example, we consider a plane wave scattering from an isotropic dielectric cube with 8 embedded bi-isotropic blocks. Both the isotropic cube with the side length of $1\lambda_0$ and bi-isotropic blocks with the side length of $0.2\lambda_0$ are with $\varepsilon_r = 2$ and $\mu_r = 1$. The center distance between two adjacent bi-isotropic blocks is $0.4\lambda_0$. Here whole structure is discretized into 8000 hexahedrons which give 27120

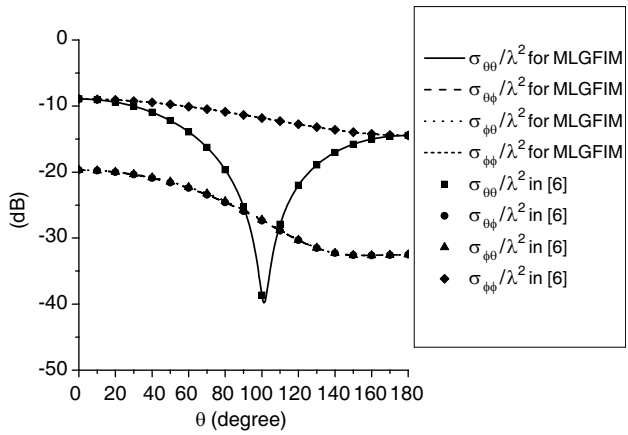

Figure 2. Plane wave scattering from homogeneous bi-isotropic cube.

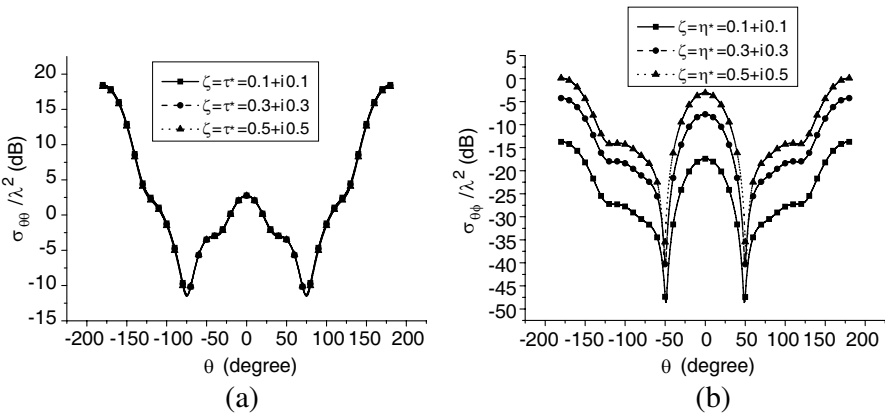

Figure 3. Plane wave scattering from an isotropic dielectric cube with 8 embedded bi-isotropic blocks: (a) co-polarized bistatic RCS; (b) cross-polarized bistatic RCS.

unknowns. The co-polarized and cross-polarized bistatic RCS for normally incident plane wave are calculated, as shown in Figs. 3(a) and (b). According to Figs. 3(a) and (b), it can be seen that the co-polarized bistatic RCS almost remains unchanged and the cross-polarized one increases with the growth of ξ and τ.

In the following, we consider an object consisting of the alternating isotropic and bi-isotropic slabs, as shown in Fig. 4(a). Both height and width of the object are $0.5\lambda_0$ and the length of each slab is $0.2\lambda_0$. The isotropic and bi-isotropic media are with $\varepsilon_r = 2$ and $\mu_r = 1$. In order to model the whole structure, 2000 hexahedrons are used and therefore 9260 unknowns are produced. The MLGFIM is used to calculate the co-polarized and cross-polarized bistatic RCS for different bi-isotropic media, as shown in Figs. 4(b) and (c). Similarly, the co-polarized bistatic RCS approximately keeps unchanged and the cross-polarized one becomes increasingly large with the growth of ξ and τ.

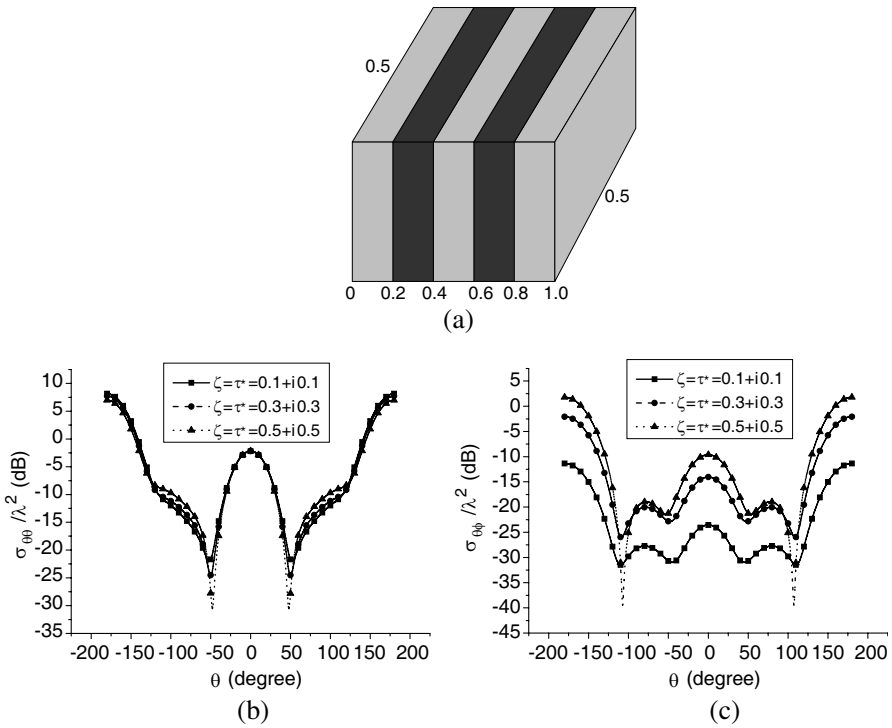

Figure 4. Plane wave scattering from an alternating isotropic dielectric and bi-isotropic structure: (a) geometry, (b) bistatic RCS with $\theta\theta$ polarization; (c) bistatic RCS with $\theta\phi$ polarization.

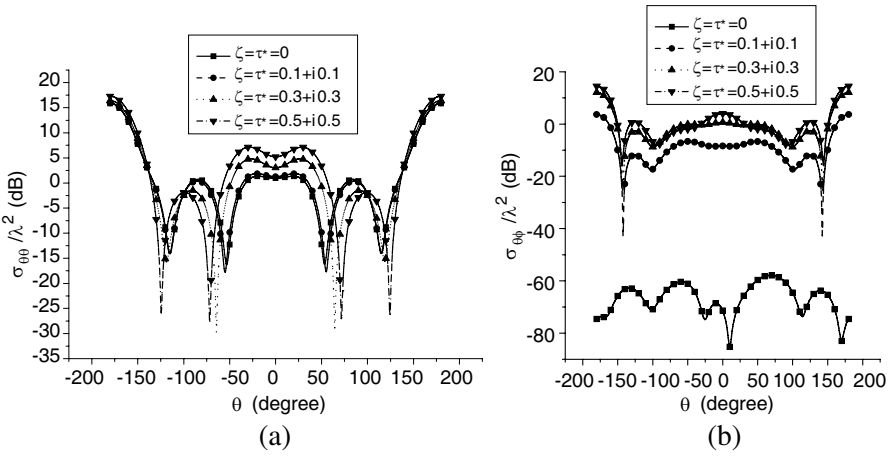

Figure 5. Plane wave scattering from a bi-isotropic cylinder shell with a PEC inner surface: (a) bistatic RCS with $\theta\theta$ polarization; (b) bistatic RCS with $\theta\phi$ polarization.

Finally, a plane wave is normally incident on a bi-isotropic cylinder shell with a PEC inner surface. The outer and inner radius of cylinder shell are $0.75\lambda_0$ and $0.25\lambda_0$, respectively and its height is $0.5\lambda_0$. Here, 6410 hexahedrons and 320 patches are used to discretize the cylinder shell and PEC surface, respectively and the resultant number of unknowns is 41630. The bi-isotropic medium is with $\varepsilon_r = 2$ and $\mu_r = 1$. Figs. 5(a) and (b) show the co-polarized and cross-polarized bistatic RCS for different bi-isotropic media. According to Figs. 5(a) and (b), the co-polarized and cross-polarized bistatic RCS increase with the growth of ξ and τ.

4. CONCLUSION

In this paper, the MLGFIM is proposed to solve electromagnetic scattering from arbitrary objects comprised of both conducting and bi-isotropic objects. The problem is formulated using volume integral equation (VIE) in terms of volume electric and magnetic flux densities for inhomogeneous bi-isotropic objects and surface integral equation (SIE) in terms of surface electric current density for conducting bodies. The application of MLGFIM significantly reduces the memory requirement and the computational complexity to $O(N)$ and $O(N \log N)$, respectively. Numerical examples were presented to illustrate the accuracy and versatility of the proposed method.

ACKNOWLEDGMENT

This work is supported partly by the National Natural Science Foundation of China under Contract No. 60801040 and No. 60601028, and partially supported by the Program for New Century Excellent Talents in University of China, National Key Laboratory Foundation, Fundamental Research Funds for the Central Universities, and the China Scholarship Council (CSC). The authors would like to thank Prof. C. H. Chan for providing this work with helpful suggestions.

REFERENCES

1. Lindell, I. V., A. H. Sihvola, S. A. Tretyakov, and A. J. Viitanen, *Electromagnetic Waves in Chiral and Bi-isotropic Media*, Artech House, Norwood, MA, 1994.
2. Serdyukov, A., I. Semchenko, S. Treyakov, and A. Sihvola, *Electromagnetics of Bi-anisotropic Materials Theory and Applications*, Gordon and Breach Science Publishers, Amsterdam, 2001.
3. Bohren, C. F., "Light scattering by an optically active sphere," *Chem. Phys. Lett.*, Vol. 29, 458–462, 1974.
4. Bohren, C. F., "Scattering of electromagnetic waves by an optically active cylinder," *J. Colloid Interface Sci.*, Vol. 66, 105–109, 1978.
5. Worasawate, D., J. R. Mautz, and E. Arvas, "Electromagnetic scattering from an arbitrarily shaped three-dimensional homogeneous chiral body," *IEEE Trans. Antennas Propagat.*, Vol. 51, 1077–1084, 2003.
6. Wang, D. X., E. K. N. Yung, R. S. Chen, and P. Y. Lau, "An efficient volume integral equation solution to EM scattering by complex bodies with inhomogeneous bi-isotropy," *IEEE Trans. Antennas Propagat.*, Vol. 55, 1970–1980, 2007.
7. Semichaevsky, A., A. Akyurtlu, D. Kem, D. H. Werner, and M. G. Bray, "Novel BI-FDTD approach for the analysis of chiral cylinders and spheres," *IEEE Trans. Antennas Propagat.*, Vol. 54, 925–932, 2006.
8. Akyurtlu, A. and D. H. Werner, "A novel dispersive FDTD formulation for modeling transient propagation in chiral metamaterials," *IEEE Trans. Antennas Propagat.*, Vol. 52, 2267–2276, 2004.
9. Sharma, R. and N. Balakrishnan, "Scattering of electromagnetic waves from arbitrary shaped bodies coated with a chiral material," *Smart Mater. Struct.*, Vol. 7, 851–866, 1998.
10. Ghaffar, A. and Q. A. Naqvi, "Study of focusing of field

refracted by a cylindrical plano-convex lens into a uniaxial crystal using Maslov's method," *Journal of Electromagnetic Waves and Applications*, Vol. 22, No. 5–6, 665–679, 2008.

11. Lu, C. C. and W. C. Chew, "A multilevel algorithm for solving a boundary integral equation of wave scattering," *Microw. Opt. Tech. Lett.*, Vol. 7, 456–461, 1994.
12. Song, J. M., C. C. Lu, and W. C. Chew, "Multilevel fast multipole algorithm for electromagnetic scattering by large complex objects," *IEEE Trans. Antennas Propagat.*, Vol. 45, 1488–1493, 1997.
13. Yang, M. L. and X. Q. Sheng, "Parallel high-order FE-BI-MLFMA for scattering by large and deep coated cavities loaded with obstacles," *Journal of Electromagnetic Waves and Applications*, Vol. 23, No. 13, 1813–1823, 2009.
14. Chew, W. C., J. M. Jin, E. Michielssen, and J. M. Song, *Fast and Efficient Algorithms in Computational Electromagnetics*, Artech House, Norwood, MA, 2001.
15. Bleszynski, E., M. Bleszynski, and T. Jaroszewicz, "AIM: Adaptive integral method for solving large-scale electromagnetic scattering and radiation problems," *Radio Sci.*, Vol. 31, 1225–1251, 1996.
16. Ling, F., C. F. Wang, and J. M. Jin, "An efficient algorithm for analyzing large-scale microstrip structures using adaptive integral method combined with discrete complex image method," *IEEE Trans. Microw. Theory Tech.*, Vol. 48, 832–837, 2000.
17. Hu, L., L. W. Li, and T.-S. Yeo, "Analysis of scattering by large inhomogeneous bi-anisotropic objects using AIM," *Progress In Electromagnetics Research*, Vol. 99, 21–36, 2009.
18. Chan, C. H., C. M. Lin, L. Tsang, and Y. F. Leung, "A sparse-matrix/canonical grid method for analyzing microstrip structures," *IEICE Trans. Electron*, E80-C, 1354–1359, 1997.
19. Li, S. Q., Y. X. Yu, C. H. Chan, K. F. Chan, and L. Tsang, "A sparse-matrix/canonical grid method for analyzing densely packed interconnects," *IEEE Trans. Microw. Theory Tech.*, Vol. 49, 1221–1228, 2001.
20. Phillips, J. R. and J. K. White, "A precorrected-FFT method for electrostatic analysis of complicated 3-D structures," *IEEE Trans. Comput. Aided Des. Integr. Circuits Syst.*, Vol. 16, 1059–1072, 1997.
21. Nie, X. C., N. Yuan, L. W. Li, Y. B. Gan, and T. S. Yeo, "A fast volume-surface integral equation solver for scattering from

composite conducting-dielectric objects," *IEEE Trans. Antennas Propagat.*, Vol. 52, 818–824, 2005.

22. Wang, H. G., C. H. Chan, and L. Tsang, "A new multilevel Green's function interpolation method for large-scale low-frequency EM simulations," *IEEE Trans. Comput. Aided Des. Integr. Circuits Syst.*, Vol. 24, 1427–1443, 2005.
23. Wang, H. G. and C. H. Chan, "The implementation of multilevel Green's function interpolation method for full-wave electromagnetic problems," *IEEE Trans. Antennas Propagat.*, Vol. 55, 1348–1358, 2007.
24. Li, L., H. G. Wang, and C. H. Chan, "An improved multilevel Green's function interpolation method with adaptive phase compensation for large-scale full-wave EM simulation," *IEEE Trans. Antennas Propagat.*, Vol. 56, 1381–1393, 2008.
25. Shi, Y., H. G. Wang, L. Li, and C. H. Chan, "Multilevel Green's function interpolation method for scattering from composite metallic and dielectric objects," *J. Opt. Soc. Am. A*, Vol. 25, 2535–2548, 2008.
26. Shi, Y. and C. H. Chan, "Multilevel Green's function interpolation method for analysis of 3-D frequency selective structures using volume/surface integral equation," *J. Opt. Soc. Am. A*, Vol. 27, 308–318, 2010.
27. Shi, Y. and C. H. Chan, "Solution to electromagnetic scattering by Bi-isotropic media using multilevel Green's function interpolation method," *Progress In Electromagnetics Research*, Vol. 97, 259–274, 2009.
28. Graglia, R. D., D. R. Wilton, and A. F. Peterson, "Higher order interpolatory vector bases for computational electromagnetics," *IEEE Trans. Antennas Propagat.*, Vol. 45, 329–342, 1997.
29. Saad, Y. and M. Schultz, "GMRES: A generalized minimal residual algorithm for solving non symmetric linear systems," *SIAM J. Sci. Stat. Comput.*, Vol. 7, 856–869, 1986.
30. Horn, R. A. and C. R. Johnson, *Topics in Matrix Analysis*, Cambridge University Press, New York, 1991.
31. Xie, Y., J. He, A. Sullivan, and L. Carin, "A simple preconditioner for electric-field integral equations," *Microw. Opt. Technol. Lett.*, Vol. 30, 51–54, 2001.